

Excess energy emission by active regions

A. Ortiz

Dept. d'Astronomia i Meteorologia, Universitat de Barcelona, Barcelona, Spain

V. Domingo

Institut d'Estudis Espacials de Catalunya, Barcelona, Spain
Space Science Dept. of ESA, ESTEC, Noordwijk, The Netherlands

B. Sanahuja

Dept. d'Astronomia i Meteorologia, Universitat de Barcelona, Barcelona, Spain
Institut d'Estudis Espacials de Catalunya, Barcelona, Spain

T. Appourchaux

Space Science Dept. of ESA, ESTEC, Noordwijk, The Netherlands

L. Sánchez

ESA/Space Science Dept. at NASA/GSFC, Greenbelt, MD, U.S.A.

C. Fröhlich

Physikalisch-Meteorologisches Observatorium Davos, World Radiation Center, Davos-Dorf, Switzerland

T. Hoeksema

H.E.P.L., Center for Space Science and Astrophysics, Stanford University, Palo Alto, CA, U.S.A.

Abstract. We study an isolated active region that crossed the solar disk during the 1996 minimum of activity. Its passage during several Carrington Rotations, specifically from rotation 1911 to 1916, allows us to analyze the evolution of the angular distribution of the excess radiance of the facular region using SOHO/VIRGO and MDI data. We associate this evolution with the evolution of the extension corresponding to the isolated active region as well as with the aging of the region itself. Finally, we evaluate the total (i.e. in all directions) emission of this facular region and its spectral and temporal evolution.

Introduction

There is a large consensus on the fact that a very large fraction of the solar irradiance variations with time are induced by the presence and evolution of the sunspots and faculae over the solar disk and probably by the photospheric network, or small features of the magnetic field [i.e., Foukal and Lean, 1986; Solanki, 1994; Fröhlich and Lean, 1998]. Most of the evidence has been obtained by statistical treatment of observations and the utilization of proxy data, such as plage and longitudinal magnetic field along the line of sight in the photosphere. Progress in the understanding of the variation of the solar energy output needs studying the radiative components associated with photospheric magnetic field features in active regions and outside them [Topka et al., 1992 and 1997].

Steiniger et al. (1996) have studied the energy balance of the emissions by active regions from a combination of direct measurements from space and ground observatories proxies. In this paper we present a first example of observation of irradiance from a single active region.

Near the minimum of solar activity in 1996, there was a time when only one, or at most two active regions, were apparent on the solar disk. The observation of a single active region over several disk passages provides a unique opportunity to study the evolution of the excess radiance produced by an evolving active region. We analyze the relationship between the evolution of the radiance of the active region, the evolution of the photospheric magnetic field and the total solar irradiance variations using data from the VIRGO and MDI instru-

ments on board the SOHO satellite.

The VIRGO instrument [Fröhlich et al., 1995] measures the total solar irradiance as well as the spectral solar irradiance at three wavelength bands. VIRGO incorporates the Low-resolution Oscillations Imager (LOI), a telescope that produces an image of the sun at 500 nm, over a 16-pixel detector, four of which are used for image stabilization. In addition, the SOI-MDI instrument [Scherrer et al., 1995] obtains solar magnetograms and radiance measurements, at 676.8 nm (continuum around the Ni I spectral line), with two arc-seconds pixel resolution.

Data

The following sets of SOHO data have been used. From MDI:

- (a) Full-disk line-of-sight longitudinal magnetograms, (1024x1024 pixels); 15 per day.
- (b) Full-disk images (1024x1024 pixels), in the intensity continuum at 676.8 nm; 4 per day.

From VIRGO:

- (c) Total solar irradiance (TSI) measured by the radiometers; hourly averages.
- (d) Spectral irradiance measured by the sunphotometers (SPMs), at 402, 500, and 862 nm; once per minute.
- (e) Spectral radiance at 500 nm in the 12 scientific pixels of LOI; once per minute. The measurements of the pixels are limited to about 70° in heliocentric angle because the outer ring of the LOI solar image is cut by the four guiding pixels.

The MDI magnetograms have been used to determine the characteristics of the magnetic active region. The MDI images in spectral radiance intensity have been used to determine the presence of sunspots.

The study of the total and spectral irradiance has been made with the VIRGO data. The angular and spectral distribution has been obtained from the TSI and SPM data, and the longitudinal extension of the emissions by the active region has been obtained from the LOI data.

Copyright 1999 by the American Geophysical Union.

Paper number GAI96112.
1524-4423/99/0103-0112\$18.00/1

The online version of this paper was published August 13, 1999.
URL: <http://eos.wdcb.rssi.ru/ijga/GAI96112/GAI96112.htm>
Print companion will be issued

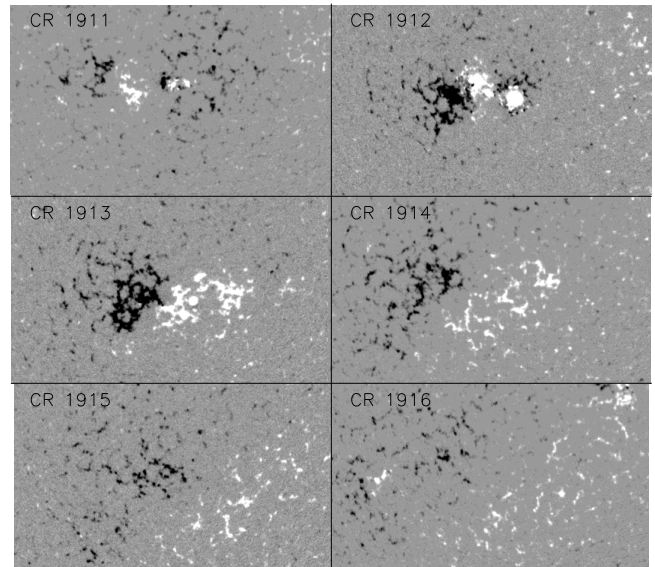


Figure 1. Solar magnetograms (line-of-sight magnetic field intensity) obtained by the MDI instrument.

Observations

During Carrington Rotation (CR) 1909, an active region, AR hereafter, appeared around Carrington longitude 250° and lasted for several solar rotations. In CR 1911 a new center of magnetic activity emerged a few heliocentric degrees away from the center of the previous AR. This center develops into a new region that it is still well visible on CR 1916. During a large part of this time interval there are no significant sunspots; in fact, rotations 1913, 1914 and 1915 are particularly sunspot free. These rotations have been used to determine the contribution of the faculae of the region and its evolution with age.

Figure 1 shows this active region, which lies between Carrington longitudes 250° and 270° . This figure presents an ensemble of MDI/SOHO magnetograms, from CR 1911 to CR 1916, each centered on the active region. The smooth aging of the region from one Carrington rotation to the next is clearly seen, as well as that its extension grows with time. During CR 1912 and CR 1913 two different active regions coexist, and there is a transition from a previous active region to a new one during CR 1911. The active region contains sunspots and faculae, only visible on the limbs; only one small sunspot is still visible in CR 1913 and has vanished in CR's 1914 and 1915.

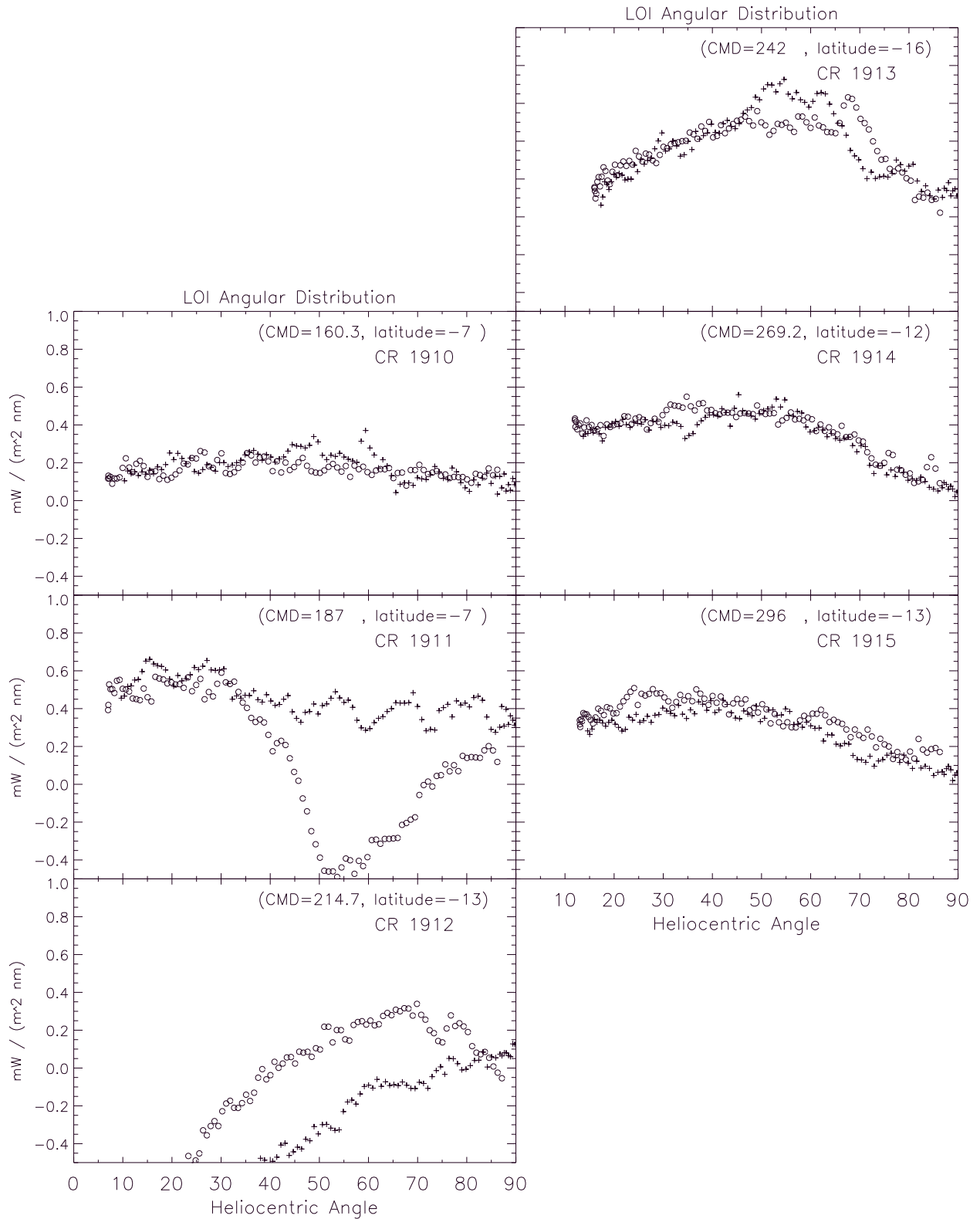


Figure 2. Angular distribution of the 500 nm spectral radiance emission from the AR observed during CR 1910 through CR 1915. The abscissa represents the heliocentric angle of the center of the AR at the moment of the measurement. The different points are obtained for each CR as the AR crosses the solar disk from East to West. Points obtained while the AR was east of the central meridian are represented by a “+”, and points obtained when it was west of the central meridian by a “o”. CMD is the day of the Central Meridian passage.

Evolution of the Angular Distribution

We have centered our analysis in the facular region and its associated excess of irradiance, consequently the presence of a sunspot is interpreted as a distortion in the observations. Figure 2 shows the evolution of the angular distribution of the excess spectral radiance at 500 nm as measured by LOI, normalized at 1 AU. In each plot we indicate the day that the center of the active region crosses the solar central meridian and the latitude of the active region center at Central Meridian Passage.

We assume that the AR is the unique source of disturbances of the solar irradiance. The angular distribution has been calculated by representing the excess or defect of flux or radiance, with respect to the quiet Sun, versus the heliocentric angle of the center of the facular region, as it rotates from East to West. Therefore, a null value means that there is no variation related to the background level. With this representation we are converting a temporal measurement into an angular distribution of the radiance; the approximation that we make is that the intensity of emission from the facular region is practically constant through the 13 days in which the region is visible in one solar rotation. In this plot “+” and “o” signs indicate the value of the radiance when the active region is East and West, respectively, of the Central Meridian. In this way we can check how valid is the assumption that the facular region has a constant irradiance as it passes across the disk. To derive these results we have assumed a punctual facular region.

A small sunspot observed in MDI intensity continuum images during CR 1913, becomes almost imperceptible in the angular distribution plots; rotations 1913, 1914 and 1915 apparently only show an excess of radiance. The aging of the active region is clear when we take into account the evolution of the excess radiance of the facular region along these rotations: the older the region, the wider its angular distribution becomes. The limb brightening peaks near 60° for CR 1913 and goes down to 45° for CR 1915. From these plots is also evident that the variations of the solar spectral irradiance are greater at shorter wavelengths. We should keep in mind that a small contribution of the sunspot present in CR 1913 could contaminate the results.

Total Facular Emission

We have tried to reproduce the center to limb variation of the facular contribution to the solar irradiance variations by fitting phenomenological models to the angular distributions presented. Specifically, we have fitted a function of the type:

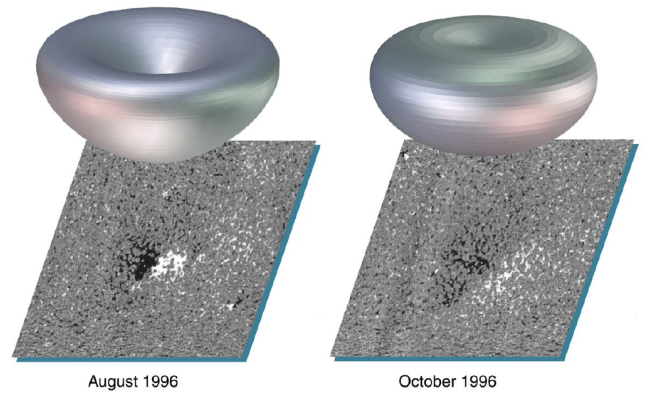


Figure 3. Three-dimensional rendering of the angular distribution of the excess irradiance emitted at 500 nm by the studied active region at two stages of its development. The brightening of the facular region is more uniform at the latter stage. The surfaces under the distributions are MDI magnetograms at the time of the CMD for the AR.

$$I(\mu) = \cos\theta(a + b \cos\theta + c \cos^2\theta) \quad (1)$$

where θ is the heliocentric angle, $\mu = \cos\theta$ and a , b and c are the limb brightening effect parameters [Chapman et al., 1992]. Rotating these curves, and assuming that the region emits the radiation in cylindrical symmetry around the vertical to the surface, we obtain a display of the excess facular emission in all directions. Figure 3 is a 3-dimensional rendering of the rotation of two of the fitted curves, corresponding to CR’s 1913 and 1915. The different angular values are obtained as the active region crosses the solar disk: from this figure one can appreciate that the angular distribution becomes less limb-brightened as the region becomes older.

Solar irradiance variations are induced, at least on time scales of a few solar rotations, by active regions which in turn are strong concentrations of magnetic flux in the solar photosphere. In figure 1 we see how the active region spreads out from CR 1913 through 1916. In CR 1912 it coexists with a former active region that had stronger magnetic field intensity. To evaluate the effect of the active region aging we develop the concept of active region extension. We use two parameters; first is the number of pixels of the active region with magnetic field intensity > 80 gauss, 7.5σ above the noise level in the MDI magnetograms (NB in figure 4). Second parameter is the AR surface, in heliocentric degrees, defined as the surface that includes 90% of the pixels with B higher than ~ 80 gauss (SAR in figure 4). Both pa-

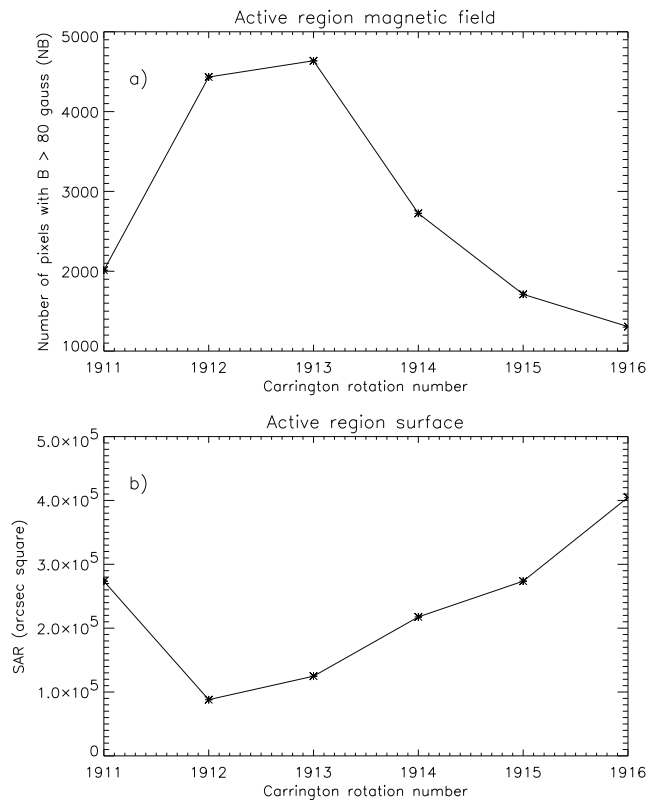


Figure 4. a) Evolution of the magnetic points: number of pixels of the active region with $B > 80$ gauss; b) Evolution of the extension of the magnetic region: area that contains 90% of the points with $B > 80$ gauss.

rameters reflect the evolution of the AR: the magnetic field of the region decays and its extension grows with time.

A facular region is composed of many small elements, which are probably individual faculae. Researchers are pursuing a detailed study of the small elements, i. e., with high-resolution images [Topka et al., 1992 and 1997]. In this study we measure the radiation emitted by the whole facular region. To compare our measurements with these observations we have assumed that the facular region is a rectangle of fixed size, this size being determined by the observations. As a first approximation, the radiation for individual faculae has been also taken of the form:

$$I(\mu) = a_i \cos \theta + b_i \cos^2 \theta + c_i \cos^3 \theta \quad (2)$$

where a_i , b_i and c_i are limb-brightening coefficients for flux tube elemental units. This radiation is integrated over the rectangle representing the active region, and this result should be similar to the angular distributions given by the VIRGO data. The coefficients for the individual faculae can be derived from integration of the

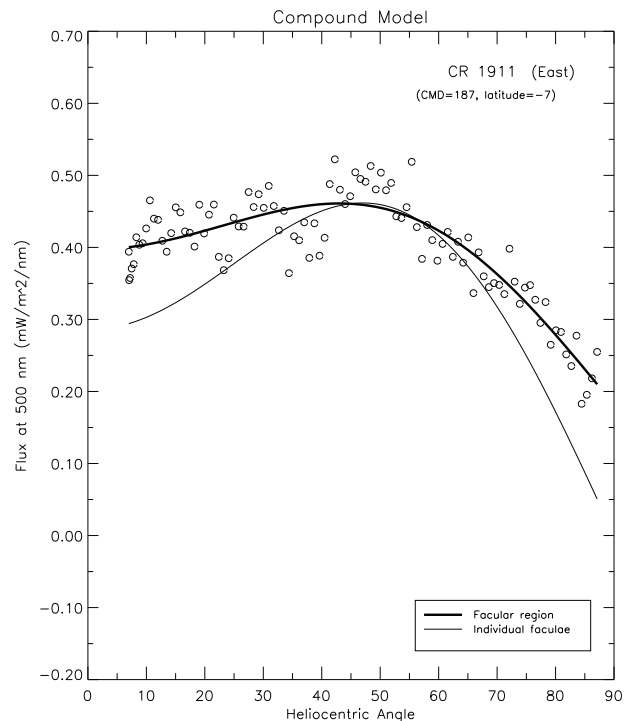


Figure 5. Observed angular distribution of the excess irradiance (circles) emitted by the AR present in CR 1911 (East of CMD) at 500 nm. The thin line is the angular distribution of the irradiance emitted by a single facula derived from the best fit to the data (thick line) when the compound model for an extended facular region is used, as described in the text.

data. An example of the obtained results is shown in figure 5; the rectangular source yields a flatter angular distribution than the individual faculae. This result is consistent with what we can expect, as the region emits from all points considered therein. For clarity, both curves have been normalized at 45° . Next step would be to consider a facular region in which elemental bright points are not uniformly distributed.

Figure 6 shows the temporal and spectral evolution of the total facular emission (volume under the 3-dimensional surface), for the three solar rotations dominated by faculae (CR's 1913, 1914 and 1915). The behaviour of the excess irradiance during CR's 1913 and 1914 is quite similar, while CR 1915 shows a decrease of the total facular emission probably due to the enlargement and spread out of the active region as it gets older. Again, the greatest excess related to the quiet Sun background occurs at the shortest wavelength (402 nm). The energy spectrum observed in this example is steeper than the spectrum for faculae reported in earlier studies [Chapman and McGuire, 1977; Lawrence, 1987; Unruh et al., 1999]. There is not a significant change in the energy spectrum with the age of the active region.

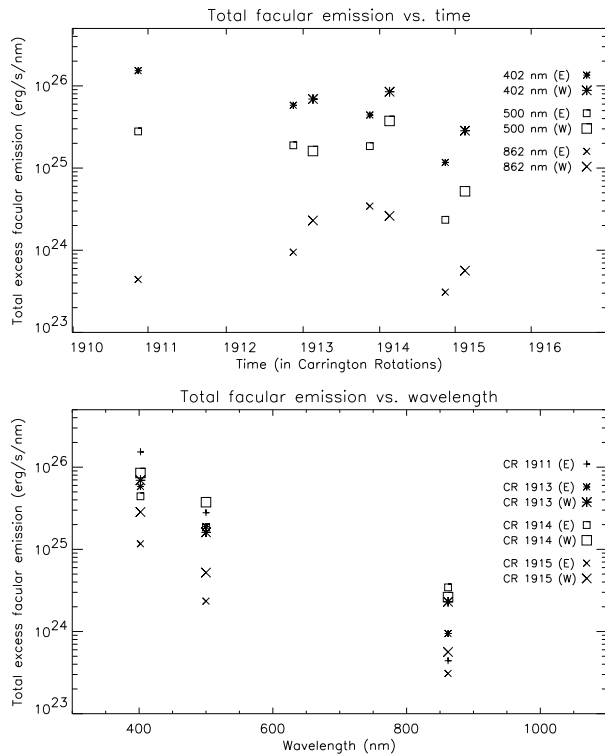


Figure 6. Top: Total spectral irradiance emitted by the active region versus time; bottom: Total spectral irradiance emitted by the active region versus wavelength. E and W mean, respectively, the East and the West disk passages of the AR.

Conclusion

The evolution of the global characteristics of the energy emission by the facular region associated with an active region that was present during several solar rotations at the minimum of solar activity has been discussed. We have studied the aging of the region using two parameters, the equivalent extension and the number of pixels with a line-of-sight photospheric magnetic field above a given magnetic threshold. The angular distribution of the excess radiance appears to reflect the increase of the extension of the magnetic active region by becoming less limb-bright as the region becomes older. A simple phenomenological model that represents this angular distribution for the facular region has been obtained as well as a tentative determination of the emission from individual faculae. The total facular emission for this sample region has been determined, showing again a relationship with the evolution of the associated magnetic field. We note that the energy spectrum is steeper than reported in previous studies and does not change much with the age of the region.

Our aim is to study more examples of emission from active regions, supported with more detailed study of the individual faculae. Further analysis will include the effect of sunspots in the irradiance variations produced by the passage of solar active regions.

References

- Chapman, G.A., A.D. Herzog, J.K. Lawrence, S.R. Walton, *J. Geophys. Res.*, Vol. 97, 1992, pp. 8211-8219.
- Chapman, G.A., T.E. McGuire, *Astrophys. J.*, Vol. 217, 1977, pp. 657-660.
- Foukal, P.J., J. Lean, *Astrophys. J.*, Vol. 328, 1986, pp. 347-357.
- Fröhlich, C. et al., *Sol. Phys.*, Vol. 162, 1995, pp. 101-128.
- Fröhlich, C., J. Lean, *Geophys. Res. Lett.*, Vol. 25, 1998, pp. 4377-4380.
- Lawrence, J.K., *Sol. Phys.*, Vol. 116, 1987, pp. 17-32.
- Scherrer, P.H. et al., *Sol. Phys.*, Vol. 162, 1995, pp. 129-188.
- Solanki, S.K., *The Sun as a Variable Star: Solar and Stellar Irradiance Variations*, Pap J., Fröhlich C., Hudson H.S., and Solanki, S.K. (eds.). IAU Colloquium 143: Cambridge Univ. Press, Cambridge, 1994, pp. 226-235.
- Steinberger, M., P.N. Brandt, H.F. Haupt, *Astron. Astrophys.*, Vol. 310, 1996, pp. 635-645.
- Topka, K.P., T.D. Tarbell, A.M. Title, *Astrophys. J.*, Vol. 396, 1992, pp. 351-363.
- Topka, K.P., T.D. Tarbell, A.M. Title, *Astrophys. J.*, Vol. 484, 1997, pp. 479-486.
- Unruh, Y.C., S.K. Solanki, M. Fligge, *Astron. Astrophys.*, Vol. 345, 1999, pp. 635-642.

(Received November 24, 1995; revised February 10, 1999; accepted July 24, 1999.)